



Methane sources in gas hydrate-bearing cold seeps: Evidence from radiocarbon and stable isotopes

J.W. Pohlman^{a,*}, J.E. Bauer^b, E.A. Canuel^b, K.S. Grabowski^c, D.L. Knies^c, C.S. Mitchell^d, M.J. Whiticar^e, R.B. Coffin^c

^a U.S. Geological Survey, Woods Hole Science Center, 384 Woods Hole Rd, Woods Hole, MA 02543, USA

^b School of Marine Science, College of Wm. & Mary, P.O. Box 1346, Gloucester Point, VA 23062, USA

^c Naval Research Laboratory, Washington D.C., 20375, USA

^d Scientific Applications International Corporation, c/o Naval Research Lab, Washington D.C., 20375, USA

^e School of Earth and Ocean Sciences, University of Victoria, P.O. Box 3055, Victoria, BC, Canada V8W 2Y2

ARTICLE INFO

Article history:

Received 9 February 2009

Received in revised form 16 June 2009

Accepted 6 July 2009

Available online 15 July 2009

Keywords:

Hydrate
Gas hydrate
Methane
Radiocarbon
Stable isotope
Cold seep
Methanogenesis

ABSTRACT

Fossil methane from the large and dynamic marine gas hydrate reservoir has the potential to influence oceanic and atmospheric carbon pools. However, natural radiocarbon (^{14}C) measurements of gas hydrate methane have been extremely limited, and their use as a source and process indicator has not yet been systematically established. In this study, gas hydrate-bound and dissolved methane recovered from six geologically and geographically distinct high-gas-flux cold seeps was found to be 98 to 100% fossil based on its ^{14}C content. Given this prevalence of fossil methane and the small contribution of gas hydrate ($\leq 1\%$) to the present-day atmospheric methane flux, non-fossil contributions of gas hydrate methane to the atmosphere are not likely to be quantitatively significant. This conclusion is consistent with contemporary atmospheric methane budget calculations.

In combination with $\delta^{13}\text{C}$ - and δD -methane measurements, we also determine the extent to which the low, but detectable, amounts of ^{14}C (~ 1 –2% modern carbon, pMC) in methane from two cold seeps might reflect *in situ* production from near-seafloor sediment organic carbon (SOC). A ^{14}C mass balance approach using fossil methane and ^{14}C -enriched SOC suggests that as much as 8 to 29% of hydrate-associated methane carbon may originate from SOC contained within the upper 6 m of sediment. These findings validate the assumption of a predominantly fossil carbon source for marine gas hydrate, but also indicate that structural gas hydrate from at least certain cold seeps contains a component of methane produced during decomposition of non-fossil organic matter in near-surface sediment.

Published by Elsevier B.V.

1. Introduction

Marine gas hydrate occurs within continental margin sediments as structural deposits near the seafloor and stratigraphic deposits in deeper regions of the gas hydrate stability zone (GHSZ) (Milkov and Sassen, 2002). Structural gas hydrate occurs near the seafloor in high-gas-flux (HGF) cold seeps where geologic features (e.g., salt diapirs and faults) provide conduits for focusing deep-sourced fluids into shallow sections of the GHSZ. By contrast, stratigraphic gas hydrate deposits occur in association with depositional features (e.g., sand layers) in which fluids accumulate by diffusive pathways (Milkov and Sassen, 2002). Recent estimates of the gas hydrate methane inventory range from 250 to 3000 Gt C (Buffett and Archer, 2004; Milkov, 2004). While globally the structural gas hydrate reservoir is believed to be smaller than that of stratigraphic gas

hydrate (Milkov, 2004), local concentrations of structural deposits typically exceed those of stratigraphic deposits (Milkov, 2005). Concentrated deposits of structural gas hydrate near the seafloor pose this reservoir to contribute potentially greater quantities of methane to the global carbon cycle (Dickens, 2003) and atmosphere (Archer, 2007) than stratigraphic deposits, especially under scenarios of increasing ocean temperatures (Levitov et al., 2005; Reagan and Moridis, 2008).

Methane in gas hydrate is a product of microbial methanogenesis and/or thermal alteration of organic matter (Whiticar, 1999). In most cases, it is possible to discern microbial and thermogenic contributions based on stable carbon isotope ratios (expressed as $\delta^{13}\text{C}$) of methane in conjunction with the relative amounts of ethane (C_2) and propane (C_3). Microbial methane is typically depleted in ^{13}C ($\delta^{13}\text{C} \leq -60\%$) relative to thermogenic methane ($\delta^{13}\text{C} \geq -50\%$) and is associated with ethane plus propane concentrations (v/v) that are less than $\sim 1\%$ of methane concentrations (Whiticar, 1999). Although exceptions to these general characteristics have been documented (e.g., Claypool et al., 1985; Milkov and Dzou, 2007; Pohlman et al., in revision), they have proven effective

* Corresponding author.

E-mail address: jpohlman@usgs.gov (J.W. Pohlman).

for identifying the sources of methane in HGF regimes where hydrocarbon gases are hypothesized to migrate rapidly along structural features to form near-seafloor gas hydrate deposits (Milkov, 2005).

In contrast to $\delta^{13}\text{C}$, the radiocarbon (^{14}C) content (expressed herein as percent modern carbon, or pMC) of methane provides information about the age of the SOC from which it was derived, rather than the process by which it was synthesized. For example, thermogenic methane generated exclusively from deeply buried kerogen is unequivocally fossil in origin (i.e., ^{14}C -free where pMC = 0, or $\geq 50,000$ years equivalent age), whereas the pMC of microbial methane is dictated by the age of the precursor SOC supporting methanogenesis. Both “old” and “new” microbial methane (Cicerone and Oremland, 1988) have been substantiated by findings of ^{14}C -depleted microbial methane from northern peatlands (Chanton et al., 1995) and marine sediments (Kessler et al., 2008). Differentiating old from new sources of microbial methane at active marine cold seeps therefore provides an opportunity to estimate the relative contributions of migrated vs. locally-generated methane within structural gas hydrate accumulations.

In this study, we present ^{14}C , $\delta^{13}\text{C}$ and δD results for gas hydrate-bound and gas hydrate-associated methane from six geologically and geographically diverse HGF cold seeps and significantly expand the existing ^{14}C database for gas hydrate methane. We further evaluate the standing assumption that the global reservoir of gas hydrate-associated methane is fossil (i.e., Cicerone and Oremland, 1988) and, by extension, that any contribution of marine gas hydrate methane to the atmosphere is also fossil (Lelieveld et al., 1998; Judd, 2004; Kvenvolden and Rogers, 2005). Delineating the sources of fossil methane is also important for establishing what fraction of the global fossil methane flux ($110 \text{ Tg CH}_4 \text{ yr}^{-1}$) is attributable to anthropogenic inputs, e.g., coal mining and petroleum production (Kvenvolden and Rogers, 2005), vs. potential dissociation of gas hydrate as ocean temperatures increase (Reagan and Moridis, 2008). Currently, the assumption of a fossil methane gas hydrate reservoir is limited to ^{14}C measurements of hydrate-bound microbial methane from Hydrate Ridge (Winckler et al., 2002) and the Santa Barbara Basin (Kessler et al., 2008). We also demonstrate in the present study that a fraction of the methane contained within structural gas hydrate from some active cold seeps is produced *in situ* by near-seafloor methanogenesis, rather than exclusively from fossil methane migrating from greater sediment depths.

2. Methods

2.1. Field sites and sampling

Fifteen gas hydrate and eight sediment core gas samples from six geographically distinct locations and various sediment horizons were collected during expeditions to six different cold seep sites between June 2000 and October 2004 (Table 1; Fig. 1). The samples were collected from the Pacific, Atlantic and Gulf of Mexico ocean margins representing a variety of geologic settings (e.g., mud volcanoes, diapirs and accretionary margins; see Table 1). All sites are HGF settings that share the general characteristic of having structural gas hydrate deposits at relatively shallow sediment depths (0–5 m below the seafloor, mbsf) (Ginsburg et al., 1999; Sassen et al., 1999; Van Dover et al., 2003; Pohlman et al., 2005;

Sellanes et al., 2005; Riedel et al., 2006). Among the samples analyzed in this study is the first gas hydrate recovered from the Chilean Margin.

Gas hydrate samples were collected by piston and gravity coring to sediment depths less than ~5 mbsf from the research vessels CCGS *John P Tully* (northern Cascadia margin: NCM), R/V *Cape Hatteras* (Blake Ridge: BR), R/V *Vidal Gormaz* (central Chilean margin: CCM) and R/V *Akademik Mstislav Keldysh* (Norwegian Sea: NS), or in pressure cylinders using the research submersibles ROPOS (NCM) and *Johnson Sea-Link* (Gulf of Mexico: GoM) (Table 1; Fig. 1). Gas hydrate samples were transferred into 60 ml gas-tight plastic syringes and allowed to dissociate at ambient temperature (Hovland et al., 1995). Core gas samples (i.e., sediment gas voids that formed within the core liner from porewater dissolved gases during core depressurization and temperature rise) were obtained by piercing expansion cracks in the clear core liner and withdrawing the gas with a plastic syringe (Hovland et al., 1995). The hydrate-bound and core gas samples were transferred to 50 ml glass serum vials, sealed with 1 cm thick butyl septa and stored at -20°C until analysis.

2.2. Analytical methods

2.2.1. Hydrocarbon composition

The hydrocarbon gas composition of the samples was determined using a Shimadzu GC 14-A gas chromatograph (GC) equipped with a PorapLOT-Q stainless steel column (8 ft, 1/8" OD) and flame ionization detector. The initial oven temperature was held at 50°C for 2 min and then ramped at $20^\circ\text{C min}^{-1}$ to a final temperature of 150°C until the C_5 hydrocarbons eluted. Hydrocarbons were identified and quantified using the retention times and peak area responses, respectively, from certified hydrocarbon gas standards.

2.2.2. Stable isotope ($\delta^{13}\text{C}$ and δD) analyses

Stable carbon and deuterium isotope ratios of methane were measured with a Finnigan Delta Plus XL isotope ratio mass spectrometer (IRMS). Methane was separated from the gas matrix by GC with a $30 \text{ m} \times 0.32 \text{ mm}$ GSQ PLOT column (initial temperature 30°C , held for 2 min and ramped at 20°C/min to 180°C). For the carbon isotope analyses ($\delta^{13}\text{C}-\text{CH}_4$), the chromatographically separated CH_4 was oxidized to CO_2 in a combustion oven (Cu/Pt at 900°C), which was interfaced to the IRMS and measured as m/z 44, 45 and 46. For the hydrogen isotope ratio analyses ($\delta\text{D}-\text{CH}_4$), the separated CH_4 was pyrolyzed at 1440°C to molecular hydrogen (H_2 gas) and carbon, and then measured by IRMS as m/z 2 and 3 (Whiticar and Eek, 2001). The carbon and hydrogen isotope ratios are reported in standard delta notation ($\delta^{13}\text{C}$ and δD , respectively) relative to the VPDB and VSMOW standards, respectively. The precision (expressed as $\pm 1\sigma$) for $\delta^{13}\text{C}-\text{CH}_4$ was $\pm 0.2\%$ and for $\delta\text{D}-\text{CH}_4$ was $\pm 1\%$.

2.2.3. Methane radiocarbon (^{14}C) analysis

2.2.3.1. Laboratory procedures. Gas samples for methane radiocarbon analysis were processed into graphite for AMS analysis at the Naval Research Lab using a cryogenic distillation, combustion and catalytic reduction apparatus (Pohlman et al., 2000), which is a modification of a

Table 1
Gas hydrate sample locations in the present study.

Region	Location	Geologic setting	Site	Latitude	Longitude	Water depth (m)
North Pacific Ocean	Northern Cascadia Margin (NCM)	Accretionary prism	Bullseye Vent	N 48° 40.07'	W 126° 50.00'	1282
			Barkley Canyon	N 48° 18.66'	W 126° 04.00'	857
Southeast Pacific Ocean	Central Chilean Margin (CCM)	Slope basin	Concepción Methane Seep	S 36° 21.87'	W 73° 43.28'	850
Northern Gulf of Mexico	Green Canyon (GC)	Fault related mud volcano	GC 185 (Bush Hill)	N 27° 46.96'	W 91° 30.48'	590
			GC 234	N 27° 44.76'	W 91° 13.32'	590
Mid-Atlantic Bight	Blake Ridge (BR)	Passive margin contourite	Blake Ridge Diapir	N 32° 29.63'	W 76° 11.52'	2177
North Atlantic Ocean	Norwegian Sea (NS)	Mud volcano	Haakon Mosby Mud volcano	N 72° 00.07'	E 14° 43.27'	1261

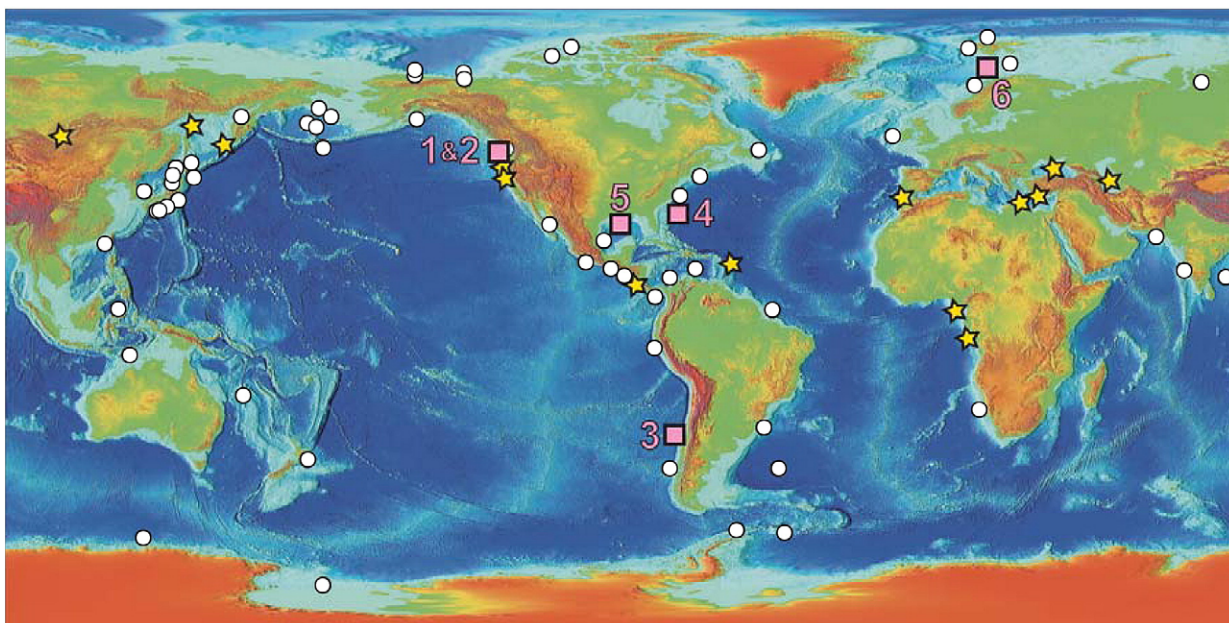


Fig. 1. Global distribution of known offshore gas hydrate occurrences. White dots indicate stratigraphic occurrences and yellow stars indicate structural occurrences in high-gas flux (HGF) setting (modified from Milkov, 2005). Pink boxes indicate where gas hydrate samples were collected for this study – 1: Bullseye vent, northern Cascadia margin; 2: Barkley Canyon, northern Cascadia margin; 3: Concepción methane seep, central Chilean margin; 4: Blake Ridge diapir; southeastern North American continental margin; 5: Green Canyon, northern Gulf of Mexico; and 6: Haakon Mosby mud volcano, Norwegian Sea. (For interpretation of the references to colour in this figure legend, the reader is referred to the web version of this article.)

system described by Chanton et al. (1992). Samples were injected into an in-line vial (see (a) in Fig. 2) through which an ultra-high purity (UHP) oxygen-enriched (20% v/v) He carrier stream (100 ml/min) flowed. Methane was cryogenically distilled from associated carbon dioxide and C₂–C₃ hydrocarbons by passing the sample through a multi-loop stainless steel trap (b) in Fig. 2) immersed in liquid nitrogen (LN₂).

The purified methane was oxidized to CO₂ over 0.5% Pt on 1/8" alumina pellets in a 650 °C furnace ((c) in Fig. 2). The methane-derived CO₂ was dried by passing it through a dry ice/ethanol multi-loop trap ((d) in Fig. 2) and then trapped in an adjacent multi-loop trap immersed in LN₂ ((e) in Fig. 2). After isolating the trap from the carrier stream and evacuating the residual He, O₂ and other non-condensables, the CO₂ was

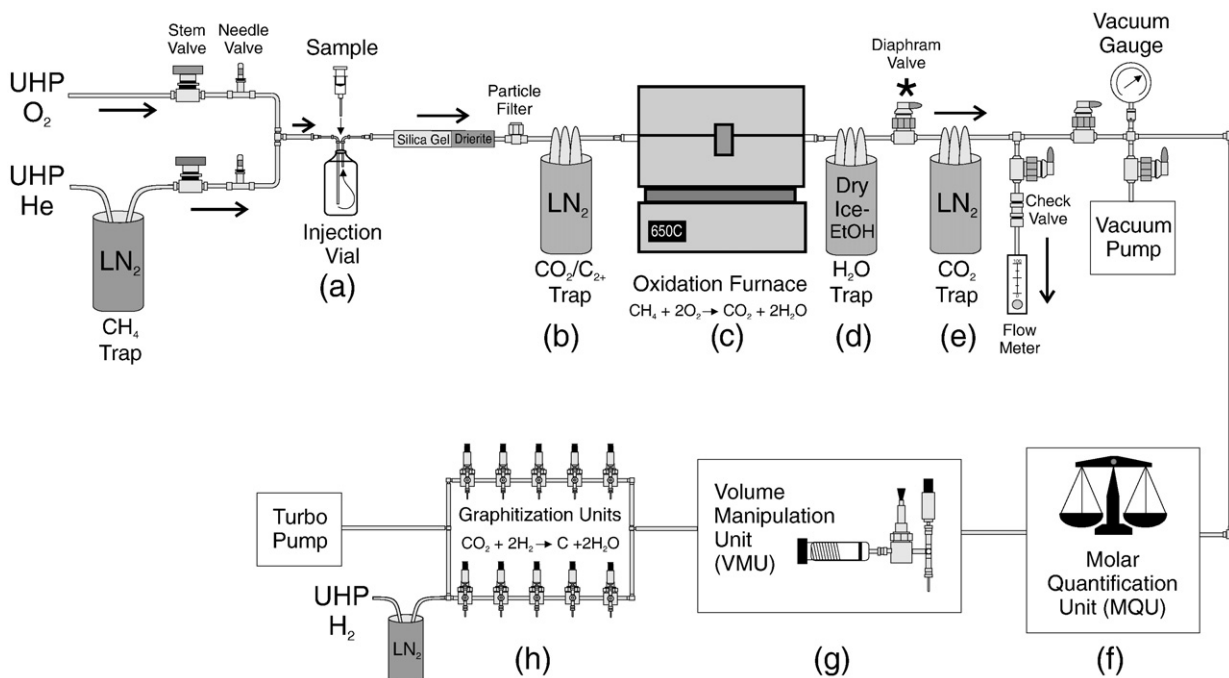


Fig. 2. Multi-stage gas sample preparation unit for radiocarbon sample preparation. The unit includes components for cryogenically distilling methane from gas mixtures, oxidizing the methane to CO₂ gas, quantifying the amount oxidized, and reducing selected volumes of CO₂ into graphite for AMS analysis. In sequence, the unit consists of components for sample injection (a), methane purification (b), oxidation (c), methane-derived CO₂ purification (d), and trapping of methane-derived CO₂ (e). Arrows indicate the direction of gas flow. After trapping, the CO₂ is isolated from the carrier stream (isolation valve indicated with asterisk) and cryogenically transferred to the Molar Quantification Unit (MQU) (f). A selected volume (1000 μg C for this study) of CO₂ is parsed from the sample with the volume manipulation unit (VMU) (g) and transferred to a graphitization unit (h) where it is reduced to graphite. LN₂: liquid nitrogen; EtOH: ethanol.

cryogenically transferred to the molar quantification unit (MQU; (f) in Fig. 2) where the mass of the CO₂ was measured by manometry. The sample was then cryogenically transferred to the volume manipulation unit (VMU; (g) in Fig. 2) where 1000 (±10) µg C (as CO₂) was isolated and transferred to a graphitization unit ((h) in Fig. 2). For additional details regarding the MQU and VMU see Pohlman et al. (2000). Within the graphitization unit (h), CO₂ was converted to graphite by iron-catalyzed reduction with ultra-high purity H₂ gas (Vogel et al., 1984).

To evaluate the performance of the gas preparation system, we measured the trapping efficiency of CO₂ from the carrier stream and the methane oxidation efficiency through the furnace. For the CO₂ trapping efficiency test, the mass of CO₂ carbon in a 2.0 ml volume was measured with a UIC Model 5011 CO₂ coulometer and determined to be 975 ± 7 µg. The carbon recovery from an equivalent volume introduced at the injection vial (a) and trapped at the MQU (f) was 969 ± 6 mg, which is indistinguishable from the coulometer calibrated injection volume. The methane oxidation efficiency was determined by introducing 2.0 ml volumes of CO₂ and methane separately into the injection vial ((a) in Fig. 2) and comparing the carbon mass recovery from each with a CO₂ coulometer connected to the flow meter downstream of the CO₂ trap ((e) in Fig. 2). The CO₂ injection recovery (947 ± 7 µg; n = 3) was indistinguishable from the methane injection recovery (945 ± 6 µg; n = 3), indicating complete oxidation of methane to CO₂. The ~28 µg C mass recovery difference between the trapping and the oxidation efficiency experiments may be due to slight temperature and pressure variations in the laboratory on the days the experiments were conducted.

2.2.3.2. Accelerator mass spectrometry (AMS). The graphite produced by the reduction of CO₂ from sample methane oxidation was pressed into aluminum targets and analyzed by AMS at the Naval Research Lab (Grabowski et al., 2000). Radiocarbon values for the samples are reported as percent modern carbon (pMC) relative to the National Institute of Standards and Technology (NIST) oxalic acid II standard (Stuiver and Polach, 1977) with an analytical precision of 0.1 to 0.4 pMC. The process blank (the total amount of exogenous carbon introduced during sample preparation) was determined from radiocarbon-free methane prepared with each set of samples. Relative to radiocarbon-free reactor grade graphite analyzed during the AMS analysis, the blanks had a ¹⁴C content of 1.04 ± 0.48 pMC (n = 9) measured across three AMS sample wheels. Among numerous possible sources for the blank signal are system leaks, sample carryover, impurities in the He, O₂ or H₂ gases that were not removed by the LN₂ traps and contamination of the blank. Assuming the ¹⁴C present in the 1000 µg methane blanks was derived from a modern carbon source (i.e., 100 pMC), the average process blank was 10.4 ± 4.8 µg C (n = 9, Table 2), which is similar to an average contribution of 8.32 µg C for a 96.1 pMC process blank reported for a field-portable methane preparation system described by Kessler et al. (2005). By applying the Grubbs' test (Grubbs, 1969) to the process blank data, we determined with 99.5% certainty that a single process blank containing 20.9 µg of blank carbon was an outlier. With that outlier removed, the standard deviation (1σ for the process blanks was 0.12 pMC (n = 8, Table 2). Samples with a pMC less than 1σ of the accepted blanks are indicated as being "indistinguishable from the blank" (Table 3). Samples with a pMC less than twice that standard deviation (2σ), but greater than 1σ are reported with an apparent pMC in Table 3 (Stuiver and Polach, 1977).

3. Results and discussion

3.1. Gas hydrate as a source of fossil methane to the oceans and atmosphere

The present study was designed to directly measure the radiocarbon content of gas hydrate-associated methane to evaluate the general assumption that gas hydrate is a global source of fossil (¹⁴C-free) carbon (Lelieveld et al., 1998; Reeburgh, 2007). Previously, direct support for gas hydrate methane being exclusively fossil was limited to measurements from a hydrate-bound sample with a ¹⁴C content of 0.2 to 0.3 (±0.1) pMC

(Winckler et al., 2002) and a sediment-hydrate slurry with methane containing 0.29 ± 0.02 pMC (Kessler et al., 2008). The ranges in radiocarbon content of methane across all sites investigated in this study range from the limit of detection (0.12 pMC) to 1.48 pMC for hydrate-bound methane, and from the limit of detection to 2.24 pMC for core gas methane (Table 3). In comparison, the radiocarbon content of atmospheric methane is ~120 to 123 pMC (Wahlen et al., 1989). Excluding Bullseye vent, the gas hydrate-bound methane from all other examined sites was less than 0.3 pMC (n = 12) (Table 3). Thus, five of our six study sites confirm the fossil nature of hydrate methane as reported and proposed by others (Winckler et al., 2002; Reeburgh, 2007; Kessler et al., 2008). Assuming that the six sites sampled in the present study and those of the previous studies are representative of the global gas hydrate reservoir, the assumption that the ~5 Tg gas hydrate methane contribution to the 500 Tg yr⁻¹ global annual atmospheric methane flux (Reeburgh, 2007) is fossil (Lelieveld et al., 1998) appears justified.

3.2. Radiocarbon evidence for shallow sedimentary methanogenesis in gas hydrate sediments

Stable isotope ratios (δ¹³C-CH₄ and δD-CH₄) and the relative abundance of higher hydrocarbon gases (i.e., ≥C₂) are both routinely used to delineate the potential sources of methane from microbial and thermogenic processes (Bernard et al., 1978; Whiticar, 1999). Using radiocarbon as an additional tracer for constraining both the process and depth of methane generation within HGF gas hydrate systems may be effective in cases where the SOC contributes measurable amounts of radiocarbon to the methane pool. The presence of ¹⁴C in methane associated with gas hydrate indicates the methane carbon originated from relatively shallow, non-fossil SOC. Furthermore, because the temperatures required for thermogenic methane production (>80 °C) generally occur at depths where the SOC is fossil (Hunt, 1996) and where gas hydrate is unstable (Sloan and Koh, 2007), we may also infer that any non-fossil fraction of methane sequestered in gas hydrate was most likely synthesized microbially. Thus, the low, but measurable, pMC for methane recovered from Bullseye vent and Barkley Canyon (Table 3), although deemed insignificant as a source of non-fossil carbon to the atmosphere (see Section 3.1), nonetheless suggests a microbial contribution from non-fossil SOC at these sites.

To estimate contributions of methane carbon from near-surface, non-fossil SOC to the hydrate-bound and core gas methane pools, we consider the gas hydrate and core gas data from Bullseye vent and employ a radiocarbon isotopic mass balance approach (Eq. (1)) using the equation

$$f_{\text{shallow}} = \frac{pMC_{\text{in-situ}} - pMC_{\text{deep}}}{pMC_{\text{shallow}} - pMC_{\text{deep}}}, \quad (1)$$

where f_{shallow} is the fractional contribution of methane generated from SOC in near-surface sediments, $pMC_{\text{in-situ}}$ is the measured pMC of the *in*

Table 2
Methane blank data for the present study.

AMS ID	Process blank (µg C) ^a	pMC ^b
NRL-425	5.2	-0.26 ± 0.23
NRL-435	9.1	0.13 ± 0.17
NRL-444	8.1	0.03 ± 0.15
NRL-452	20.9	1.3 ± 0.20 ^c
NRL-453	8.9	0.11 ± 0.16
NRL-466	11.8	-0.04 ± 0.15
NRL-476	11.8	-0.02 ± 0.22
NRL-491	12.8	0.08 ± 0.18
NRL-1149	5.2	0.00 ± 0.09
Average	10.4 ± 4.8 µg	0.00 ± 0.12 (1σ) ^d

^a Exogenous carbon acquired during sample preparation.

^b Corrected for process blank.

^c Identified as an outlier by the Grubbs' test ($p < 0.005$).

^d Excludes outlier.

Table 3
Hydrocarbon and isotopic composition of gas hydrate-bound and associated core gas.

Location and gas source	Cruise/dive	AMS ID	¹⁴ C [pMC]	δ ¹³ C-CH ₄ [‰]	δD-CH ₄ [‰]	C ₁ [%]	C ₂ [%]	C ₃ [%]	i-C ₄ [%]	n-C ₄ [%]	^a ΣC ₅ [%]
Bullseye Vent, Northern Cascadia Margin (NCM)											
Gas hydrate	PGC0208	NRL-456	1.48 ± 0.24	-64.6	-178	99.8	0.21	b.d.	b.d.	b.d.	b.d.
	PGC0208	NRL-458	1.47 ± 0.28	-63.2	-173	99.9	0.13	<0.01	b.d.	b.d.	b.d.
	PGC0208	NRL-467	i.f.b.	-63.8	-175	99.7	0.24	0.04	0.02	0.03	b.d.
Core gas	PGC0208	NRL-454	2.24 ± 0.27	-79.3	-172	>99.9	0.01	<0.01	b.d.	b.d.	b.d.
	PGC0208	NRL-455	2.20 ± 0.39	-77.8	-177	>99.9	0.06	<0.01	b.d.	b.d.	b.d.
	PGC0208	NRL-460	1.68 ± 0.31	-67.7	-145	>99.9	0.06	<0.01	b.d.	b.d.	b.d.
Barkley Canyon, Northern Cascadia Margin (NCM)											
Gas hydrate	PGC0208	NRL-433	i.f.b.	-44.7	-167	81.9	7.8	5.9	2.0	1.8	0.45
	R694	NRL-431	0.28 ± 0.37	-43.4	-143	85.1	7.7	3.3	1.1	1.7	0.67
	R694	NRL-472	i.f.b.	-42.6	-139	81.9	10.4	3.8	1.2	2.0	0.5
	R694	NRL-473	i.f.b.	-42.9	-138	84.3	9.1	3.3	1.0	1.7	0.55
	R695	NRL-439	[0.16 ± 0.17]	-42.7	-140	68.1	10.8	12.5	4.2	2.2	1.51
	PGC0208	NRL-442	0.85 ± 0.21	-45.1	-183	97.3	1.63	0.60	0.31	0.14	<0.01
Core gas	PGC0208	NRL-459	1.17 ± 0.20	-44.9	-180	97.0	1.87	0.63	0.30	0.15	0.03
Concepción Methane Seep, Central Chilean Margin (CCM)											
Gas hydrate	CHL1004	NRL-1152	i.f.b.	-61.4	n.a.	>99.9	0.03	<0.01	b.d.	b.d.	b.d.
Core gas	CHL1004	NRL-1147	i.f.b.	-61.7	n.a.	>99.9	0.02	<0.01	b.d.	b.d.	b.d.
	CHL1004	NRL-1150	[0.14 ± 0.11]	-62.5	n.a.	>99.9	0.05	<0.01	b.d.	b.d.	b.d.
	CHL1004	NRL-1151	i.f.b.	-63.1	n.a.	>99.9	0.04	b.d.	b.d.	b.d.	b.d.
Green Canyon, Northern Gulf of Mexico (GoM)											
Gas hydrate	4220,GC234	NRL-468	i.f.b.	-49.5	-192	62.3	8.7	19.4	6.3	1.4	1.7
	4216,GC234	NRL-477	i.f.b.	-48.8	-179	68.3	12.6	12.2	3.4	2.1	0.66
	4211,GC185	NRL-478	i.f.b.	-44.7	-205	67.8	11.4	14.2	3.4	2.5	0.52
Blake Ridge Diapir, Blake Ridge (BR)											
Gas hydrate	BR2002	NRL-470	i.f.b.	-66.5	-186	>99.9	0.09	<0.01	b.d.	b.d.	b.d.
	BR2002	NRL-471	i.f.b.	-65.3	-187	>99.9	0.08	<0.01	b.d.	b.d.	b.d.
Haakon Mosby Mud Volcano, Norwegian Sea (NS)											
Gas hydrate	HMMV00	NRL-469	i.f.b.	-63.2	-209	>99.9	0.04	<0.01	b.d.	b.d.	b.d.

^aΣC₅: *i*-pentane + *n*-pentane + *neo*-pentane.

i.f.b.: indistinguishable from blank; <0.12 pMC (1σ), see text for details.

[]: apparent pMC; 0.12(1σ) < pMC < 0.24 (2σ), see text for details.

b.d.: below detection.

n.a.: not analyzed.

situ methane, pMC_{deep} is the pMC of deep-sourced, fossil methane and pMC_{shallow} is the pMC of methane generated from SOC in the near-surface methanogenic zone. The average radiocarbon contents of hydrate-bound methane ($pMC_{\text{in-situ}} = 0.98 \pm 0.85$; $n = 3$, Table 3) and core gas methane ($pMC_{\text{in-situ}} = 2.04 \pm 0.31$; $n = 3$, Table 3) from the Bullseye vent site were used to represent the radiocarbon content of the methane associated with the near-seafloor structural gas hydrate accumulations. The deep methane end-member (pMC_{deep}) was assumed to have a pMC = 0, and the pMC of the shallow microbial methane end-member (pMC_{shallow}) was represented by the pMC of the associated SOC. The average pMC of SOC for ten samples from three piston cores sampled to a maximum sediment depth of 5.73 mbsf at the Bullseye vent site was 10.1 ± 3.0 pMC (Pohlman, 2006) and is used here as pMC_{shallow} in the mass balance estimates.

The estimated contribution of methane produced from SOC in the upper 5.73 mbsf is 7.5 to 13.8% when using the gas hydrate methane end-member and 15.6 to 28.7% when using the core gas methane end-member. These estimates confirm that gas hydrate-associated methane in HGF settings may be formed by *in situ* processes occurring near the site of gas hydrate nucleation in structural settings (Milkov, 2005; Milkov et al., 2005). In addition, while the locally-generated gas hydrate methane reported by Milkov et al. (2005) was produced at sediment depths of 50–105 mbsf, our results extend the depth range from which a fraction of the gas hydrate formed near the seafloor is comprised of locally-generated methane to the upper 5 mbsf.

That the gas hydrate-associated methane contained measureable amounts of non-fossil methane at the northern Cascadia margin sites (Bullseye vent and Barkley Canyon) may be a consequence of rapid sediment accumulation during the termination of the Last Glacial Maximum (LGM). Rapid sediment accumulation enhances the preservation of organic matter by limiting its temporal exposure to

aerobic and anaerobic diagenesis (Bernier, 1980); thereby making the SOC that is eventually converted to methane more labile. Furthermore, rapid burial of the SOC places it within the methanogenic zone during the ~50,000 yr time window when ¹⁴C exists. The radiocarbon age of planktonic foraminifera from near-surface (<6 mbsf) sediments at Bullseye vent site range from 14,850 to 16,100 yr B.P. (Pohlman, 2006); a time interval that coincides with the Late Wisconsin Glacial Maximum and early stage of deglaciation (Blaise et al., 1990). Production and melting of icebergs during that time released large quantities of ice rafted debris, which supported exceptional sedimentation rates ranging from 76 to 162 cm ka⁻¹ (Blaise et al., 1990). By comparison, sedimentation during the Holocene at another nearby site was only ~5 cm ka⁻¹ (McKay et al., 2004) and sedimentation rates on the crest of Blake Outer Ridge were ~4.2 cm ka⁻¹ during the Late Pleistocene (Okada, 2000).

Other seeps on the northern Cascadia margin and continental margins that experienced rapid sedimentation during the past 50,000 yrs may also provide radiocarbon-based evidence of locally-generated, hydrate-associated methane. For example, glacial melting in the high-Andes mountains after the LGM produced exceptionally high sedimentation rates of 265 cm ka⁻¹ along some parts of the Peru margin (Skilbeck and Fink, 2006) that may have placed non-fossil terrigenous SOC in the methanogenic zone of seeps in that area (e.g., Torres et al., 1996). However, any process that rapidly buries and preserves organic matter (e.g., high primary production in upwelling zones, turbidite deposition, and large flood events) can place non-fossil SOC within the methanogenic zone. Furthermore, in places of slower sediment deposition, where the SOC is fossil, but still metabolizable, *in situ* methanogenesis may also contribute a fraction of the methane associated with the near-surface structural gas hydrate. However, in such cases, ¹⁴C cannot be used as evidence for the process.

3.3. Application of methane radiocarbon signatures for spatial and process-based gas source classification

The gas samples (both hydrate-bound and core gas) from Barkley Canyon and Green Canyon (Table 1, Fig. 1), sites that occur in geologic settings with known thermogenic petroleum systems (Sassen et al., 1999; Pohlman et al., 2005), contained 62 to 97% methane and $\delta^{13}\text{C}\text{-CH}_4$ values that ranged from -42.9% to -49.5% (Table 3). These values are typical of a thermogenic gas source (Whiticar, 1999). By contrast, gases from the other locations (Bullseye vent, Concepción methane seep, Blake Ridge diapir and Haakon Mosby mud volcano; Table 1, Fig. 1) were essentially pure methane (>99.7%) and had more negative $\delta^{13}\text{C}\text{-CH}_4$ values of -61.4% to -79.3% (Table 3), indicative of a microbial gas source (Whiticar, 1999). The distinction between thermogenic and microbial sources is illustrated by plotting the hydrocarbon gas composition expressed as the Bernard ratio, $C_1/(C_2 + C_3)$ (Bernard et al., 1978), against the corresponding average $\delta^{13}\text{C}\text{-CH}_4$ from each site (Fig. 3).

Methane radiocarbon data provide additional information for interpreting the sources and spatial origins of gas hydrate-associated methane. Non-fossil core gas methane carbon (average pMC = 1.01; $n = 2$, Table 3) from the thermogenic-dominated Barkley Canyon site (Fig. 4) provides direct evidence for an additional microbial methane contribution from non-fossil OM, which is consistent with the evidence for a 20% microbial contribution at this site as determined by the natural gas plot model (Pohlman et al., 2005). For the Concepción seep, Blake Ridge diapir and Haakon Mosby mud volcano, seeps with microbially sourced hydrate-associated methane, the pMC of methane was, in all but one case, indistinguishable from the process blank (Table 3). Possible explanations for this observation are that the SOC in the upper methanogenic region was fossil in nature, or that the flux of a deep, fossil microbial source dominated the near-surface methane reservoir. However, these scenarios cannot be resolved without knowledge of the ^{14}C content of the SOC at each location.

At Bullseye vent, the hydrate-bound methane had a lower pMC and was ^{13}C -enriched relative to the core gas methane (Fig. 4). The lower pMC of the hydrate-bound methane suggests a partial contribution from a lower pMC source and/or radioactive decay of ^{14}C within the hydrate phase, while the ^{13}C -enriched signature of the hydrate phase methane suggests a partial contribution from a ^{13}C -enriched source and/or oxidation within the hydrate phase (e.g., Sassen et al., 1999). Isotopic fractionation of ^{13}C during gas hydrate formation does not

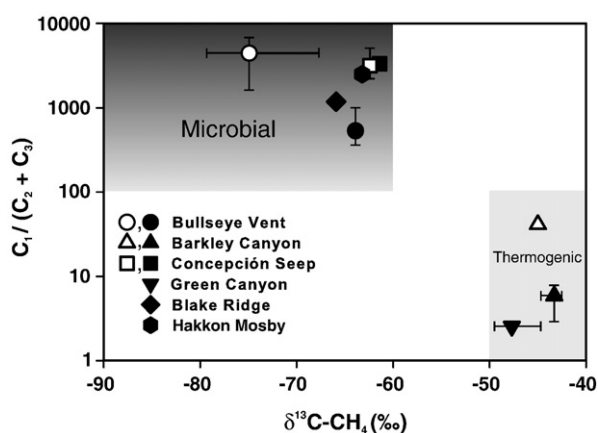


Fig. 3. Characterization of thermogenic and microbial gas sources of methane from gas hydrate-bound (filled symbols) and the core gas samples (open symbols) based on the hydrocarbon composition $[C_1/(C_2 + C_3)]$ and $\delta^{13}\text{C}\text{-CH}_4$ values, as defined by Bernard et al. (1978). The horizontal and vertical bars respectively indicate the range of $\delta^{13}\text{C}\text{-CH}_4$ and Bernard ratios for the present study. Where bars are absent, the symbols either represent a single sample or the range of values is less than the size of the symbol (see Table 3 for data).

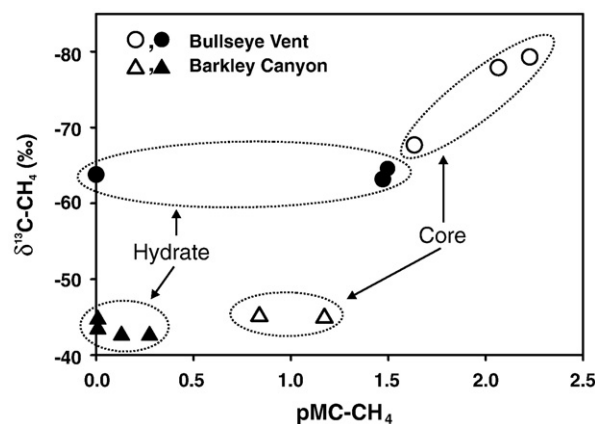


Fig. 4. Relationship between the $\delta^{13}\text{C}$ and percent modern carbon (pMC) values of methane from gas hydrate-bound (filled symbols) and core gas samples (open symbols) for the northern Cascadia margin study sites, Bullseye vent (circles) and Barkley Canyon (triangles). Distinct clustering of the core gas and hydrate-bound methane data at each site suggests these gas reservoirs are not in isotopic equilibrium. Higher pMC values in the core gas methane from both sites suggest a greater near-seafloor microbial methane contribution. At Bullseye vent, where thermogenic contributions are insignificant, the more positive $\delta^{13}\text{C}$ values in the hydrate-bound methane suggest a greater contribution from depth-migrated, ^{13}C -enriched microbial methane. Temporal variations in the gas flux and sources that have charged each reservoir are suggested as an explanation for the isotopic disequilibrium.

occur (Sassen et al., 1999; Pohlman et al., 2005) and, thus, did not likely influence the isotopic differences between the hydrate-bound and core gas phases.

To constrain mechanisms for the distinct $\delta^{13}\text{C}$ and pMC signatures of methane at Bullseye vent, we also considered the δD signatures of the methane. Microbial methane oxidation within gas hydrate has been suggested to enrich the residual hydrate-bound methane in both D and ^{13}C (Sassen et al., 1999). The $\sim 11\%$ enrichment in $\delta^{13}\text{C}$ of the hydrate-bound methane from Bullseye vent ($-63.9 \pm 0.7\%$; $n = 3$, Table 3) relative to the free-gas methane ($-75.0 \pm 6.3\%$; $n = 3$, Table 3) is consistent with more extensive microbial oxidation in the hydrate-bound methane. However, the δD of the gas hydrate-bound methane ($-175 \pm 3\%$; $n = 3$, Table 3) and the core gas methane ($-165 \pm 17\%$; $n = 3$, Table 3) are indistinguishable, which is inconsistent with an oxidation effect. That is, more extensive methane oxidation within gas hydrate would be expected to produce more positive hydrate-bound δD methane values. Therefore, the $\delta^{13}\text{C}$ and pMC disparities between the hydrate-bound and core gas methane at Bullseye vent (Fig. 4; Table 3) most likely arise as a result of spatiotemporal variations in deep and shallow gas contributions.

An interpretation consistent with the ^{13}C , ^{14}C and δD data from Bullseye vent is that the hydrate-bound methane contains a greater quantity of fossil and simultaneously ^{13}C -enriched deep-sourced methane than the core gas representing the local dissolved pool. The origin of the deep-sourced methane may be thermogenic or microbial. However, in the absence of an exceptionally "dry" thermogenic gas source, the near-absence of thermogenic hydrocarbons ($\text{C}_3\text{-C}_5$; Table 3) precludes a substantial thermogenic contribution. A more realistic scenario is that the fossil and ^{13}C -enriched gas hydrate methane has a greater contribution of microbial methane that has migrated from a deeper reservoir. Methane migrated from depth will certainly be fossil. Furthermore, the $\delta^{13}\text{C}$ of microbial methane in continental margin settings is known to become more ^{13}C -enriched with increasing depth as a result of a methanogenic kinetic isotope effect during sediment burial (Galimov and Kvenvolden, 1983; Claypool et al., 1985; Paull et al., 2000; Pohlman et al., in revision). We speculate that the disparity between the ^{14}C and ^{13}C content of the hydrate-bound and core gas is the result of *in situ* production of non-fossil, ^{13}C -depleted methane that has

not fully equilibrated with the migrated fossil and ^{13}C -enriched gas hydrate-bound methane.

3.4. 3-source model for HGF gas hydrate-bearing cold seeps

The potential sources for gas hydrate-associated methane in HGF systems are: 1) migrated microbial methane, 2) microbial methane produced near the site of hydrate nucleation and 3) a deep thermogenic reservoir (Milkov, 2005). By incorporating methane radiocarbon signatures as an additional source indicator, we demonstrate unequivocally that an *in situ* source contributes methane to structural gas hydrate accumulations near the seafloor (e.g., <5 mbsf) of an active cold seep. A conceptual model that incorporates our findings with Milkov's (2005) 3-source model summarizes potential methane sources for structural gas hydrate within HGF cold seep systems and exchange pathways between the seep, the water column and the atmosphere (Fig. 5). In some systems, thermogenic methane generated from catagenesis of fossil OM migrates from the deep subsurface to form accumulations of structural gas hydrate near the seafloor. Microbial methane produced from below the base of the gas hydrate stability zone also migrates upward and is supplemented with additional microbial inputs during vertical migration. In systems where the SOC within the methanogenic zone contains some non-fossil carbon, ^{14}C in the hydrate-bound methane provides direct evidence that methane synthesized near the seafloor is a constituent of structural gas hydrate systems. Additionally, the ^{14}C -depleted nature of methane carbon in HGF gas hydrate may be utilized as a natural tracer for investigating the cycling of methane carbon within the greater ocean–atmosphere system as well as within hydrate-bearing sediments of continental margins.

4. Conclusions

The radiocarbon (^{14}C) content of methane from structural gas hydrate and associated sediments from six geographically diverse sites with HGF regimes was found to be between 98% and 100% fossil. These findings significantly expand the global geographic range of gas hydrate methane ^{14}C measurements and support previous studies that suggest the marine gas hydrate methane reservoir and contributions of methane from that reservoir to the atmosphere are largely fossil. In addition, we estimate that ~8–14% of the gas hydrate-bound methane and ~16 to 29% of the dissolved methane associated with gas hydrate from Bullseye vent on the northern Cascadia margin could be generated by microbial processing of non-fossil sediment organic carbon in the vicinity of shallow (<5 mbsf) structural gas hydrate accumulations. The recognition that the globally significant gas hydrate reservoir is dominantly, but not entirely, fossil may help to more accurately constrain our understanding of how methane from gas hydrate systems influences the isotopic signatures and radiocarbon ages of major ocean carbon reservoirs (i.e., DOC and DIC), the processes by which the methane in the gas hydrate systems is synthesized, and the depths over which these processes occur.

Acknowledgements

This work was supported by the Office of Naval Research, the Naval Research Laboratory (NRL) and Geological Survey of Canada. We thank the numerous scientists, engineers, captains and crew members who facilitated the collection of samples aboard the vessels CCGS *John P Tully*, R/V *Cape Hatteras*, R/V *Vidal Gormaz*, R/V *Akademik Mstislav Keldysh* and with the submersibles *ROPOS* and the *Johnson Sea-Link*. Partial support

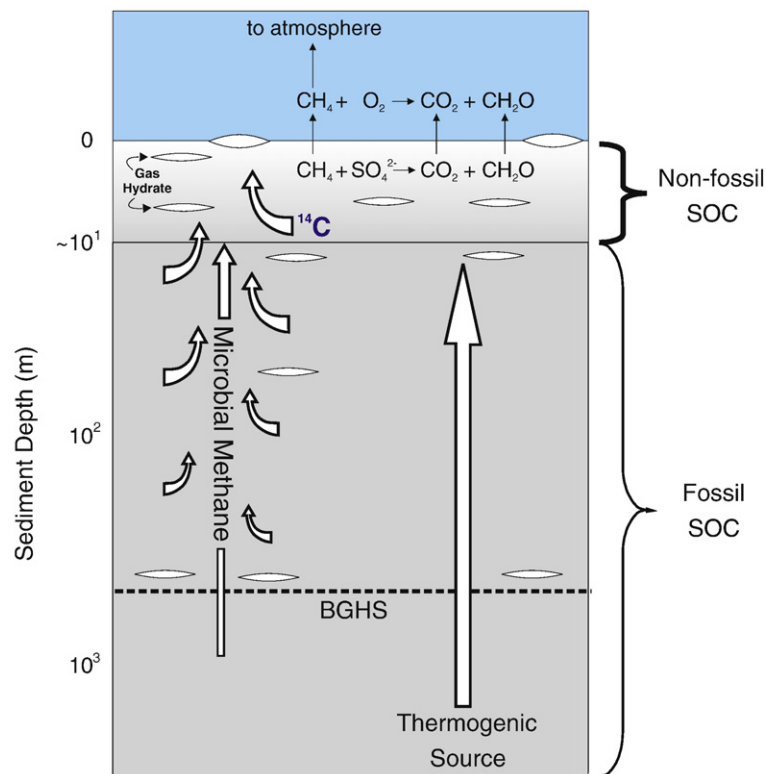


Fig. 5. Conceptual model for the sources and cycling of methane in high-gas-flux (HGF) gas hydrate systems. The potential gas hydrate gas sources are (1) deep-sourced microbial methane, (2) deep-sourced thermogenic gases and (3) microbial methane produced within the gas hydrate stability zone (GHSZ). Methane produced from sediment organic carbon (SOC) with a non-fossil component provides direct evidence for *in situ* production of methane near the seafloor. The decreasing size of arrows representing microbial contributions within the GHSZ indicates a diminishing methane production rate from the more deeply buried, increasingly-recalcitrant organic matter. Cycling of predominately fossil methane in the sediments and the water column has the potential to generate significant quantities of fossil metabolites that may alter the isotopic signatures and the radiocarbon content of ocean carbon pools. CO₂ and CH₂O generically represent the dissolved inorganic carbon (DIC) and dissolved organic carbon (DOC) pools in pore water and the deep ocean. BGHS: base of gas hydrate stability zone.

was also provided by the USGS Mendenhall Postdoctoral Research Fellowship Program to JWP, and NSF Chemical Oceanography (OCE-0327423) and Integrated Carbon Cycle Research (EAR-0403949) program support to JEB. We gratefully acknowledge Jack McGeehin and Jeff Chanton for technical advice during the development of the radiocarbon sample preparation facility at NRL, Paul Eby and Rebecca Plummer for analytical support, and Brett Renfro and Catalina Cetina for assistance with the data analysis. Carolyn Ruppel and Eric Sundquist provided valuable comments on a previous version of the manuscript. We also thank Ed Pelzer (Associate Editor) and two anonymous reviewers for constructive comments and suggestions. References to non-USGS equipment are provided for information only and do not constitute endorsement by the USGS, U.S. Department of the Interior, or U.S. Government.

References

- Archer, D., 2007. Methane hydrate stability and anthropogenic climate change. *Biogeosciences* 4, 521–544.
- Bernard, B.B., Brooks, J.M., Sackett, W.M., 1978. Light-hydrocarbons in recent Texas continental-shelf and slope sediments. *Journal of Geophysical Research-Oceans and Atmospheres* 83, 4053–4061.
- Berner, R.A., 1980. *Early Diagenesis: A Theoretical Approach*. Princeton University Press, Princeton, NJ.
- Blaise, B., Clague, J.J., Mathews, R.W., 1990. Time of maximum Late Wisconsin glaciation, west-coast of Canada. *Quaternary Research* 34, 282–295.
- Buffett, B., Archer, D., 2004. Global inventory of methane clathrate: sensitivity to changes in the deep ocean. *Earth and Planetary Science Letters* 227, 185–199.
- Chanton, J.P., Whiting, G.J., Showers, W.J., Crill, P.M., 1992. Methane flux from *Peltandra virginica*: stable isotope tracing and chamber effects. *Global Biogeochemical Cycles* 6, 15–31.
- Chanton, J.P., Bauer, J.E., Glaser, P.A., Siegel, D.I., Kelley, C.A., Tyler, S.C., Romanowicz, E.H., Lazrus, A., 1995. Radiocarbon evidence for the substrates supporting methane formation within northern Minnesota peatlands. *Geochimica et Cosmochimica Acta* 59, 3663–3668.
- Cicerone, R.J., Oremland, R.S., 1988. Biochemical aspects of atmospheric methane. *Global Biogeochemical Cycles* 2, 299–327.
- Claypool, G.E., Threlkeld, C.N., Mankiewicz, P.N., Arthur, M.A., Anderson, T.F., 1985. Isotopic composition of interstitial fluids and origin of methane in slope sediment of the Middle America Trench, Deep Sea Drilling Project Leg 84. In: von Huene, R., Aubouin, J., et al. (Eds.), *Initial Reports of the Deep Sea Drilling Project*, vol. 84. US Government Printing Office, Washington, pp. 683–691.
- Dickens, G.R., 2003. Rethinking the global carbon cycle with a large, dynamic and microbially mediated gas hydrate capacitor. *Earth and Planetary Science Letters* 213, 169–183.
- Galimov, E.M., Kvenvolden, K.A., 1983. Concentrations and carbon isotopic composition of CH₄ and CO₂ in gas from sediments of the Blake Outer Ridge. In: Sheridan, R.E., Gradstein, F.M., et al. (Eds.), *Initial Reports of the Deep Sea Drilling Project*, vol. 76. US Government Printing Office, Washington, pp. 403–417.
- Ginsburg, G.D., Milkov, A.V., Soloviev, V.A., Egorov, A.V., Cherkashev, G.A., Vogt, P.R., Crane, K., Lorenson, T.D., Khutorsky, M.D., 1999. Gas hydrate accumulation at the Hakon Mosby Mud Volcano. *Geo-Marine Letters* 19, 57–67.
- Grabowski, K.S., Knies, D.L., DeTurck, T.M., Treacy, D.J., Pohlman, J.W., Coffin, R.B., Hubler, G.K., 2000. A report on the Naval Research Laboratory AMS facility. *Nuclear Instruments and Methods in Physics Research B* 172, 34–39.
- Grubbs, F., 1969. Procedures for detecting outlying observations in samples. *Technometrics* 11, 1–21.
- Hovland, M., Lysne, D., Whiticar, M., 1995. Gas hydrate and sediment gas composition, Hole 892A. In: Carson, B., Westbrook, G.K., Musgrave, R.J., Suess, E. (Eds.), *Proc. ODP, Sci. Results*, vol. 146 (Pt. 1), Ocean Drilling Program, College Station TX, pp. 151–161. doi:10.2973/odp.proc.sr.146-1.210.1995.
- Hunt, J.M., 1996. *Petroleum Geochemistry and Geology*, 2nd edition. Freeman, New York, NY, p. 743.
- Judd, A.G., 2004. Natural seabed gas seeps as sources of atmospheric methane. *Environmental Geology* 46, 988–996.
- Kessler, J.D., Reeburgh, W.S., Southon, J., Varela, R., 2005. Fossil methane source dominates Cariaco Basin water column methane geochemistry. *Geophysical Research Letters* 32, L12609. doi:10.1029/2005GL022984.
- Kessler, J.D., Reeburgh, W.S., Valentine, D.L., Kinnaman, F.S., Peltzer, E.T., Brewer, P.G., Southon, J., Tyler, S.C., 2008. A survey of methane isotope abundance (¹⁴C, ¹³C, ²H) from five nearshore marine basins that reveals unusual radiocarbon levels in subsurface waters. *Journal of Geophysical Research-Oceans* 113, C12021. doi:10.1029/2008JC004822.
- Kvenvolden, K.A., Rogers, B.W., 2005. Gaia's breath – global methane exhalations. *Marine and Petroleum Geology* 22, 579–590.
- Lelieveld, J., Crutzen, P.J., Dentener, F.J., 1998. Changing concentration, lifetime and climate forcing of atmospheric methane. *Tellus. Series B, Chemical and Physical Meteorology* 50, 128–150.
- Levitov, S., Antonov, J., Boyer, T., 2005. Warming of the world ocean, 1955–2003. *Geophysical Research Letters* 32, L02604. doi:10.2973/2004GL021592.
- McKay, J.L., Pedersen, T.F., Kienast, S.S., 2004. Organic carbon accumulation over the last 16 kyr off Vancouver Island, Canada: evidence for increased marine productivity during the deglacial. *Quaternary Science Reviews* 23, 261–281.
- Milkov, A.V., 2004. Global estimates of hydrate-bound gas in marine sediments: how much is really out there? *Earth-Science Reviews* 66, 183–197.
- Milkov, A.V., 2005. Molecular and stable isotope compositions of natural gas hydrates: a revised global dataset and basic interpretations in the context of geological settings. *Organic Geochemistry* 36, 681–702.
- Milkov, A.V., Dzou, L., 2007. Geochemical evidence of secondary microbial methane from very slight biodegradation of undersaturated oils in a deep hot reservoir. *Geology* 35, 455–458. doi:10.1130/G23557A.1.
- Milkov, A.V., Sassen, R., 2002. Economic geology of offshore gas hydrate accumulation and provinces. *Marine and Petroleum Geology* 19, 1–11.
- Milkov, A.V., Claypool, G.E., Lee, Y.J., Sassen, R., 2005. Gas hydrate systems at Hydrate Ridge offshore Oregon inferred from molecular and isotopic properties of hydrate-bound and void gases. *Geochimica et Cosmochimica Acta* 69, 1007–1026.
- Okada, H., 2000. Neogene and Quaternary calcareous nannofossils from the Blake Ridge, Sites 994, 995, and 997. In: Paull, C.K., Matsumoto, R., et al. (Eds.), *Proc. ODP, Sci. Results*, vol. 164. Ocean Drilling Program, College Station TX, pp. 331–341.
- Paull, C.K., Lorenson, T.D., Borowski, W.S., Ussler, W., Olsen, K., Rodriguez, N.M., 2000. Isotopic composition of CH₄, CO₂ species, and sedimentary organic matter within samples from the Blake Ridge: gas source implications. In: Paull, C.K., Matsumoto, R., et al. (Eds.), *Proc. ODP, Sci. Results*, vol. 164. Ocean Drilling Program, College Station TX, pp. 67–78.
- Pohlman, J.W., 2006. *Sediment biogeochemistry of northern Cascadia margin shallow gas hydrate systems*, PhD Dissertation, College of William and Mary, p. 239.
- Pohlman, J.W., Knies, D.L., Grabowski, K.S., DeTurck, T.M., Treacy, D.J., Coffin, R.B., 2000. Sample distillation/graphitization system for carbon pool analysis by accelerator mass spectrometry (AMS). *Nuclear Instruments and Methods in Physics Research B* 172, 428–433.
- Pohlman, J.W., Canuel, E.A., Chapman, N.R., Spence, G.D., Whiticar, M.J., Coffin, R.B., 2005. The origin of thermogenic gas hydrates on the northern Cascadia Margin as inferred from isotopic (¹³C/¹²C and D/H) and molecular composition of hydrate and vent gas. *Organic Geochemistry* 36, 703–716.
- Pohlman, J.W., Kaneko, M., Heuer, V.B., Coffin, R.B., Whiticar, M. Methane sources and production patterns in the northern Cascadia margin gas hydrate system. *Earth and Planetary Science Letters* (in revision).
- Reagan, M.T., Moridis, G.J., 2008. Dynamic response of oceanic hydrate deposits to ocean temperature change. *Journal of Geophysical Research-Oceans* 113, C12023. doi:10.1029/2008JC004938.
- Reeburgh, W.S., 2007. Oceanic methane biogeochemistry. *Chemical Reviews* 107, 486–513.
- Riedel, M., Novosel, I., Spence, G.D., Hyndman, R.D., Chapman, R.N., Solem, R.C., Lewis, T., 2006. Geophysical and geochemical signatures associated with gas hydrate-related venting in the northern Cascadia margin. *Geological Society of America Bulletin* 118, 23–38.
- Sassen, R., Joye, S., Sweet, S.T., DeFreitas, D.A., Milkov, A.V., MacDonald, I.R., 1999. Thermogenic gas hydrates and hydrocarbon gases in complex chemosynthetic communities, Gulf of Mexico continental slope. *Organic Geochemistry* 30, 485–497.
- Sellanes, J., Quiroga, E., Gallardo, V.A., 2005. First direct evidences of methane seepage and associated chemosynthetic communities in the bathyl zone off Chile. *Journal of the Marine Biological Association of the United Kingdom* 84, 1065–1066.
- Skilbeck, C.G., Fink, D., 2006. Data report: radiocarbon dating and sedimentation rates for Holocene–Upper Pleistocene sediments, eastern equatorial Pacific and Peru continental margin. In: Jørgensen, B.B., D'Hondt, S.L., Miller, D.J. (Eds.), *Proc. ODP, Sci. Results*, vol. 201, pp. 1–15.
- Sloan, E.D., Koh, C.A., 2007. *Clathrate Hydrates of Natural Gases*, 3rd edition. CRC Press, Boca Raton, FL, p. 721.
- Stuiver, M., Polach, H.A., 1977. Discussion: reporting ¹⁴C data. *Radiocarbon* 19, 355–363.
- Torres, M.E., Bohrmann, G., Suess, E., 1996. Authigenic barites and fluxes of barium associated with fluid seeps in the Peru subduction zone. *Earth and Planetary Science Letters* 144, 469–481.
- Van Dover, C.L., Aharon, P., Bernhard, J.M., Caylor, E., Doerries, M., Flickinger, W., et al., 2003. Blake Ridge methane seeps: characterization of a soft-sediment, chemo synthetically based ecosystem. *Deep-Sea Research I* 50, 281–300.
- Vogel, J.S., Southon, J.R., Nelson, D.E., Brown, T.A., 1984. Performance of catalytically condensed carbon for use in accelerator mass-spectrometry. *Nuclear Instruments and Methods in Physics Research B* 233, 289–293.
- Wahlen, M., Tanaka, N., Henry, R., Deck, B., Zeglen, J., Vogel, J.S., Southon, J., Shemesh, A., Fairbanks, R., Broecker, W., 1989. Carbon-14 in methane sources and in atmospheric methane: the contribution from fossil carbon. *Science* 245, 286–290.
- Whiticar, M.J., 1999. Carbon and hydrogen isotope systematics of bacterial formation and oxidation of methane. *Chemical Geology* 161, 291–314.
- Whiticar, M.J., Eek, M., 2001. New approaches for stable isotope ratio measurements. *Proc. Advisory Group meeting held in Vienna, Sep 20–23, 1999*. International Atomic Energy Agency, pp. 75–95. IAEA-TECDOC-1247.
- Winckler, G., Aeschbach-Hertig, W., Holoher, J., Kipfer, R., Levin, I., Poss, C., Rehder, G., Suess, E., Schlosser, P., 2002. Noble gases and radiocarbon in natural gas hydrates. *Geophysical Research Letters* 29. doi:10.1029/2001GL014013.